BPTI liquid-liquid phase separation monitored by light and small-angle X–ray scattering

S. Grouazel,[a] J. Perez,[b] J.-P. Astier,[a] F. Bonneté[a] and S. Veesler[a*]

[a]*Centre de Recherche sur les Mécanismes de la Croissance Cristalline, CRMC2[#]-CNRS, Campus de Luminy, Case 913 F-13288 Marseille cedex 09, France and* [b]*LURE (CNRS-CEA-MENRT) Centre Universitaire Paris-Sud Bat 209D, B.P.34, F-91898 Orsay Cedex, France. E-mail: veesler@crmc2.univ-mrs.fr*

In the field of protein crystallization, a better knowledge of the nucleation process is essential to control the nucleation rate, the growth and therefore the size and the quality of crystals. With that aim, it becomes clear that the important stage is the determination of the protein phase diagram. We highlighted and investigated the bovine pancreatic trypsin inhibitor (BPTI) binary liquid-liquid phase separation in 350 mM KSCN solutions as a function of temperature. We measured the low concentration part of the binodal curve using light scattering and optical microscopy. We show, from small angle X-ray scattering experiments, that the high concentrated phase sediments in the bottom of the capillary and we analysed the low concentrated phase in terms of monomers/decamers equilibrium.

Keywords: BPTI, liquid-liquid phase separation, small-angle X-ray scattering

1. Introduction

One of the challenging tasks in protein crystallization is to control the nucleation rate, the objective being to obtain a few crystals in solution near the equilibrium state, in order to control the growth and therefore the size and the quality of crystals.

Recent works (Muschol & Rosenberger, 1997; Haas & Drenth, 1999) suggest that a metastable liquid-liquid (L-L) phase separation or demixing can affect nucleation. The nucleation is expected to be different above and below the coexistence or binodal curve. Experimental results and simulation calculations seem to indicate that nucleation is enhanced in the vicinity of this curve (Wolde & Frenkel, 1997; Haas & Drenth, 1999; Galkin & Vekilov, 2000).

After the work of Lafont on solubilities and "precipitation" of the bovine pancreatic trypsin inhibitor (BPTI) in KSCN solutions (Lafont *et al*., 1997), we recently found out a L-L phase separation in the BPTI phase diagram as a function of temperature and BPTI concentration in 350 mM KSCN at pH 4.9. It is the first time that this transition was observed for BPTI.

In the present work, we have characterized this BPTI L-L phase separation, using light scattering and optical microscopy. We have measured the cloud point temperature (Tc) and then determined the binodal curve of BPTI solutions in 350 mM KSCN at pH 4.9. We also present preliminary results using small angle X-ray scattering (SAXS) to put in evidence this L-L phase separation. It is now well established that BPTI particles in acidic solution are a mixture of monomers and decamers (Hamiaux *et al*., 2000). The fraction of decamers was found to increase with increasing protein concentration (Hamiaux, 2000).

The growth unit in acidic conditions is the decamer (Hamiaux *et al*., 2000; Budayova-Spano *et al*., 2002), so it is probable that nucleation kinetic is strongly related to the decamer quantity in solution. Therefore, it is interesting to follow the variation of the proportion of BPTI monomers and decamers present in solution during the L-L phase separation.

2. Materials and methods

2.1 Protein solutions

BPTI (bovine pancreatic trypsin inhibitor, 6511 Da, pI = 10.5) was supplied as a lyophilized powder by Bayer and used as received without further purification. Proper amounts of BPTI and KSCN were dissolved in pure water (ELGA UHQ reverse osmosis system) to obtain stock solutions needed for phase separation trials and SAXS experiments**.** The different solutions were buffered with acetic acid to 80 mM, adjusted to pH 4.5 with NaOH (1M) and filtered through 0.22 µm Millipore filters. After dissolution of BPTI, the pH was 4.9. The BPTI concentration was controlled by optical density measurements using an extinction coefficient of 0.786 $cm^2.mg^{-1}$ at 280 nm. In all the study, the salt concentration was fixed at 350 mM KSCN and the pH at 4.9.

2.2 Phase diagram determination

Binodal curves for the two liquid phases were determined by recording the variation of the scattering intensity at 90° (static light scattering) as a function of time and temperature. The appearance of liquid droplets when decreasing the temperature induces a jump in the scattering intensity. Hence, we note this temperature as Tc. On raising the temperature after the L-L phase separation above Tc, the cloudiness responsible for the strong signal peak readily disappeared. The experimental setup for light scattering experiments (SEM 633, Sematech-France) was previously described (Veesler *et al*., 1993). Several points were verified by a direct observation of BPTI solutions in a thermostated cell under an optical microscope (Nikon Diaphot).

2.3 Small-angle X-ray scattering

2.3.1 SAXS experiments

X-ray scattering curves were recorded on the SAXS instrument D24 using the synchrotron radiation emitted by the DCI storage ring at the Laboratory for Synchrotron Radiation, L.U.R.E. (Vachette, 1979; Boulin *et al.*, 1986; Depautex *et al.*, 1987; Dubuisson *et al.*, 1997). DCI storage ring was operated at 1.85 GeV and 320 mA. The sample-detector distances were 1605 and 1870 mm and the wavelength of the X-rays was 1.488 Å. The curves were scaled to the transmitted intensity; the background (i.e. salt-buffer signal) was subtracted from the scattering curve of BPTI-salt-buffer mixtures.

The total normalized intensity I(c,s), scattered by a solution of monodisperse spherical particles at a scattering angle 2θ, can be expressed as a function of the modulus of the scattering vector s, $s = 2\lambda^{-1}\sin\theta$, and of the particle concentration c by:

$$I(c,s) = I(0,s) \times S(c,s) \qquad (1)$$

I(0,s), the intensity scattered by one particle, is the Fourier transform of the spherically averaged auto-correlation function of the electron density contrast associated with the particle and is usually called the particle form factor (Luzzati & Tardieu, 1980). S(c,s), usually called the solution structure factor, reflects interactive effects due to attractive or repulsive interactions between particle (Tardieu, 1994).

Note, that for a polydisperse solution made of two protein oligomers, the total form factor is the sum of the form factors of the two oligomers, weighted by their respective quantities.

[#] Laboratory associated to the Universities Aix-Marseille II and III

2.3.2 Simulation procedure

Calculated form factors for BPTI monomer and decamer were obtained using CRYSOL program (Svergun *et al*., 1995) from a set of crystallographic coordinates (PDB entry 1BHC; Hamiaux *et al*., 1999). At very low angles, ($s < 0.01$ Å^{-1}), interparticle interactions may perturb the scattering intensity and affect the form factor. To minimize this effect, we will only consider the angle range from 0.01 to 0.035 Å^{-1}. The experimental curves were systematically fitted as a linear combination of monomers and decamers as described by Hamiaux (Hamiaux *et al*., 2000). For this study, the fitting curve procedure was performed using an IDL software (Research systems). For every linear combination, the fit residual χ^2 was calculated, according to the following equation:

$$\chi^2 = \frac{1}{N}\sum_{j=1}^{N}\left(\frac{y - y_j}{\sigma_j}\right)^2 \qquad (2)$$

where N is the total number of experimental points, y is the experimental value, y_j the corresponding simulated value, and $1/\sigma_j$ the weighting value, and σ_j the experimental error. The best fit corresponds to the smallest χ^2, and in every case, the plot of residuals, corresponding to a normalized difference between the experimental curve and the fit, was generated to control visually the good quality of the fit.

Two main pieces of information were taken into account for the fitting procedure: the protein quantity that contributed to the scattering of the X-rays (the sum of the mass coefficients attributed to monomer and decamer form factors, i.e. the calculated concentration), and the percentage of decamers.

3. Results

3.1. L-L phase separation and phase diagram

Figure 1 shows the appearance of droplets in a supersaturated solution of BPTI, when the temperature is decreased. The temperature of appearance of droplet is denoted Tc (the cloud point temperature) . Note that this transition is metastable, the crystal is the stable phase (the monoclinic crystal present in the micrographs was seeded prior to the demixing experiment).

Cloud point data were obtained by light scattering (Lafont *et al*., 1997 and this study). In Figure 2, solubility and cloud point data for BPTI are presented. Due to the protein solution instability with respect to crystal nucleation at high concentrations (above 120 mg.ml^{-1}), the high concentration part of the binodal curve was not established. The KSCN concentration in the low concentration phase was checked by measurement of the refractive index after the liquid-liquid phase separation, and no significant variation was found. This confirms that this is a binary L-L phase separation and not a salt repartitioning.

3.2. SAXS experiments

SAXS experiments were performed for three initial BPTI concentrations, 21, 15 and 10 mg.ml^{-1}, in the temperature range from 30 to 5°C. According to Figure 2, solutions at 21 and 15 mg.ml^{-1} lead to a binary L-L phase separation. The solution at 10 mg.ml^{-1} does not undergo a phase separation and was used as a reference for simulations. The variation of the SAXS intensity of BPTI solutions at 21 mg.ml^{-1} are plotted *versus* angle s (Å^{-1}) for temperatures ranging from 30°C to 5°C (Fig. 3). A drastic effect appeared at all angles below 20°C. From Figure 2, at 21 mg.ml^{-1} of BPTI in KSCN 350 mM, the cloud temperature is Tc = 17°C.

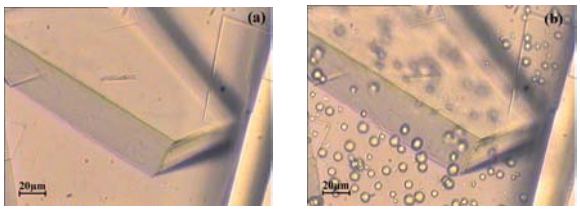

Figure 1
Observation by optical microscopy of the apparition of droplets of the protein rich phase in a supersaturated solution of BPTI (24 mg.ml^{-1}, 350 mM KSCN, pH = 4.9) when decreasing the temperature: (a) T = 20°C and (b) T = 15°C.

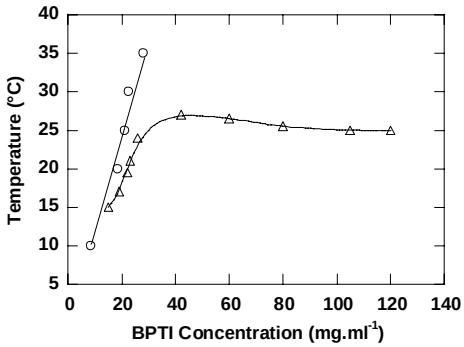

Figure 2
Phase diagram for BPTI with 350 mM KSCN. Open circles: solubility of monoclinic BPTI from Lafont *et al*., 1997. Triangles: cloud point data. Lines are only guidelines.

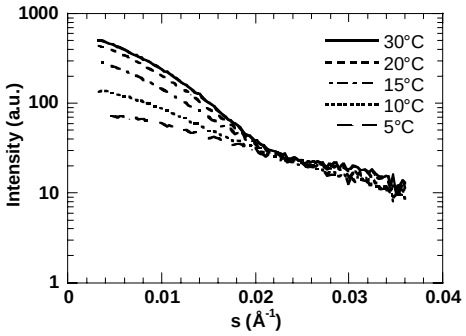

Figure 3
Evolution of SAXS curves as a function of temperature, in the range 30 to 5°C for a solution of BPTI at 21 mg.ml^{-1} with 350 mM KSCN. In this condition, the cloud temperature is Tc = 17°C. The curve recorded at 25°C is identical to that at 30°C, the dashed line corresponds to the curve recorded at 15°C. Note that no isoscattering point is observed because the represented curves are not normalised by the quantity of BPTI irradiated by X-rays, which quantity can vary (see text).

3.3. Curve fitting

Figure 4 shows the computed form factors for pure solutions of monomers and decamers, together with the mixture of monomers and decamers which displays the best agreement with the experimental curve of BPTI 21 mg.ml^{-1}, KSCN 350 mM. All results - percentage of monomers and decamers and final concentration - are

summarized with the initial concentration condition and temperature in table 1 and Figures 5 and 6. The procedure described in section 2 allows us to follow the evolution, during the experiment, of the BPTI concentration of the solution irradiated by X-rays (Fig. 5), together with the monomer/decamer proportion of BPTI proteins present in the solution after the phase separation (Fig. 6).

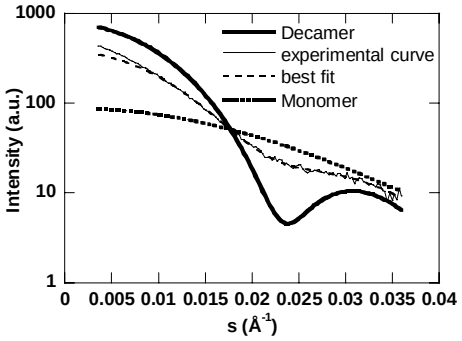

Figure 4
Calculated curves computed with CRYSOL for decamers (thick line) and monomers (dotted line), SAXS experimental curves in 350 mM KSCN at 20°C, the initial BPTI concentration was 21 mg.ml^{-1} and the best fit (dashed line) considering a mixture of 57.3% of monomers and 42.7% of decamers.

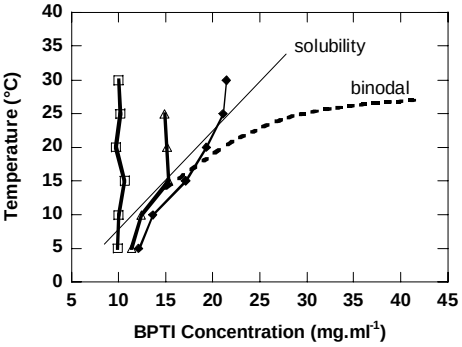

Figure 5
Evolution of the BPTI concentration of the solution irradiated by X-rays from SAXS data, *versus* temperature (see also table 1). The solubility and binodal curves are plotted *versus* temperature in order to place the experimental conditions in the phase diagram.

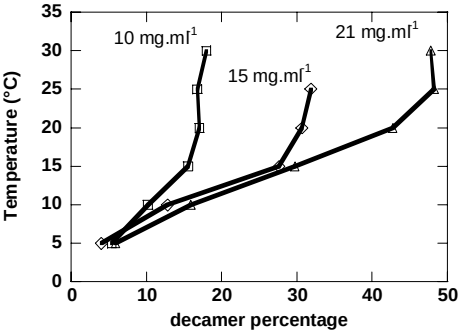

Figure 6
Evolution of the decamer percentage calculated from SAXS data, *versus* temperature (see table 1).

4. Discussion

The liquid-liquid phase separation of BPTI solutions in 350 mM KSCN at pH = 4.9 was investigated by optical microscopy observation, light scattering and SAXS experiments. When crossing the binodal curve, the solutions become cloudy and droplets appeared (Fig. 1). The fitting of the SAXS data allowed us to determine the proportion of monomer and decamer in solution and the protein concentration into the X-ray beam at different temperatures for different initial concentrations.

Table 1
Results of curve fits for each temperature and initial BPTI concentrations: weight fractions of decamer and monomer and calculated BPTI concentrations (mg.ml^{-1}).

Initial BPTI concentration 21 mg.ml^{-1}				
Temperature °C	Monomer %	Decamer %	Calculated BPTI concentration	χ^2
30	52.3	47.7	21.5	1.4
25	51.8	48.2	21.1	1.2
20	57.3	42.7	19.3	1.3
15	70.3	29.7	17.2	1.5
10	84.1	15.9	13.6	0.8
5	94.2	5.8	12.1	1.3

Initial BPTI concentration 15 mg.ml^{-1}				
Temperature °C	Monomer %	Decamer %	Calculated BPTI concentration	χ^2
25	68.2	31.8	14.9	1.1
20	69.4	30.6	15.1	1.2
15	72.4	27.6	15.3	1.1
10	87.2	12.8	12.4	1.1
5	96.0	4.0	11.4	1.1

Initial BPTI concentration 10 mg.ml^{-1}				
Temperature °C	Monomer %	Decamer %	Calculated BPTI concentration	χ^2
30	82.0	18	10.0	1.1
25	83.3	16.7	10.2	1.5
20	83.0	17.0	9.7	1.1
15	84.5	15.5	10.6	0.9
10	89.8	10.2	10.0	0.9
5	94.6	5.4	9.9	1.2

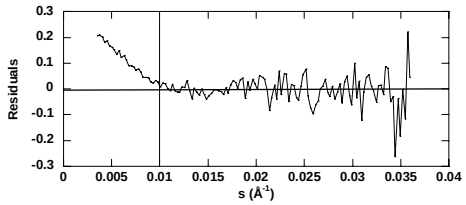

Figure 7
Plot of the fitting residuals *versus* s, for a BPTI solution at 21mg.ml^{-1} with 350 mM KSCN at pH 4.9 and 30°C. Residuals are computed following $R = (I_{exp} - I_{calc})/0.5((I_{exp} + I_{calc})$, where I_{exp} is the experimental intensity and I_{calc} is the calculated intensity obtained from fit results performed on the angle range from 0.01 to 0.035 Å^{-1}, and extrapolated to the low angle area.

To go further with the results plotted in Figure 4, we can compare experimental and calculated curves over the whole s-range, as shown in Figure 7, where the residual between experimental and calculated data are plotted. The calculated intensity is found to be weaker than the experimental data in the low s region. This confirms that, at very low angles $s < 0.01$ Å^{-1}, interparticle interactions affect the form factor. Surprisingly, for the two conditions leading to a liquid-liquid phase separation, the calculated concentrations decrease during the experiment (Fig. 5). By optical observation, no crystals

were observed in these solutions, so that the decrease of the concentration could not be explained by the nucleation and growth of crystals (note that in the experiment presented in figure 1 the crystal was seeded). The fitted concentration overlaps at and below 15°C, where both concentrations are considered to undergo liquid-liquid phase separation. At the same time, both of the fitted concentrations change along the binodal curve when the temperature is lowered, as if both solutions were the same. By contrast, for the reference solution at 10 $mg.ml^{-1}$ that did not experience liquid-liquid phase separation, the fitted concentration does not behave in a corresponding manner. All calculated concentrations meet at 5°C, and if we extrapolate the binodal, at this temperature, the corresponding binodal concentration would be 11 ± 1 $mg.ml^{-1}$. This result is confirmed by the evolution of the decamer percentages in BPTI solutions at 21 and 15 $mg.ml^{-1}$ which meet at 15°C (Fig. 6). The evolution of the decamer percentage for the reference solution is only due to the temperature variation. From these observations, we can conclude that, during the L-L phase separation, the high concentrated phase sediments in the bottom of the capillary and only the low concentrated phase remains in the X-ray beam. This result confirms that the phase separation only concerns the protein. Otherwise, if the KSCN concentration should have been significantly different in the two phases, the decamer percentage, which is highly dependent on the salt concentration (Hamiaux *et al.*, 2000) should have been different.

5. Conclusion

We evidenced and investigated the binary liquid-liquid phase separation of different BPTI solutions in 350 mM KSCN as a function of temperature. We measured the low concentration part of the binodal curve. We have shown, from SAXS experiments, that the high concentrated phase sediments in the bottom of the capillary and that only the low concentrated phase remains in the X-ray beam. The fitting of SAXS data gave the proportion of monomers and decamers in solution above and along the binodal curve.

In the future we will consider the influence of the decamer percentage and liquid-liquid phase separation on the nucleation and crystallization of BPTI.

Acknowledgements

We thank Bayer A.G. (Wuppertal, Germany) for providing us with BPTI and E.C. (Biotech program, reference BIO4-CT98-0086 DG12-SSMI) for financial support. We thank Dr P. Vachette (LURE-CNRS, Orsay), Dr S. Tanaka (AIST, Japan) for their advice in the SAXS experiments and to M.C. Toselli for technical assistance.

References

Budayova-Spano, M., Bonneté, F., Astier, J.P. & Veesler, S. (2002). *J. Cryst. Growth*, **235**, 547-554.
Boulin, C., Kempf, R., Koch, M. H. J. & McLaughlin, S. M. (1986). *Nucl. Instrum. Methods A*, **249**, 399-407.
Depautex, C., Desvignes, C., Feder, P., Lemonnier, M., Bosshard, R.,
Leboucher, P., Dageaux, D., Benoit, J. P. & Vachette, P. (1987). LURE: rapport d'activité pour la période Août 1985-1987.
Dubuisson, J. M., Decamps, T. & Vachette, P. (1997). *J. Appl. Cryst.* **30**, 49-54.
Galkin, O. & Vekilov, P.G. (2000). *Proc. Natl Acad. Sci USA*, **97**, 6277-6281.
Haas, C. & Drenth, J. (1999). *J. Cryst. Growth*, **196**, 388-394.
Hamiaux, C., Prangé, T., Riès-Kautt, M., Ducruix, A., Lafont, S., Astier, J.P. & Veesler, S. (1999). *Acta Cryst.* D**55**, 103-113.
Hamiaux, C., (2000) Thèse, Université de Paris XI U.F.R. Scientifique d'Orsay.
Hamiaux, C., Perez, J., Prangé, T., Veesler, S., Riès-Kautt, M. & Vachette, P. (2000). *J. Mol. Biol.* **297**, 697-712.
Lafont, S., Veesler, S., Astier, J.P. & Boistelle, R. (1997). *J. Cryst. Growth*, **173**, 132-140.
Luzzati, V. & Tardieu, A. (1980). *Ann. Rev. Biophys. Bioeng.* **9**, 1-29.
Muschol, M. & Rosenberger, F. (1997). *J. Chem. Phys.* **107**, 1953-1961.
Svergun, D., Barberato, C. & Koch, M. H. J. (1995). *J. Appl. Cryst.* **28**, 768-773.
Tardieu, A. (1994). *Neutron and synchrotron radiation for condensed matter studies*. Vol. III, pp 145-160. Grenoble: Springer-Verlag.
Vachette, P. (1979). Thèse, Université Louis Pasteur, Strasbourg, France.
Veesler, S., Marcq, S., Lafont, S., Astier, J.P. & Boistelle, R. (1993). *Acta Cryst.* D**50,** 355-360.
Wolde, P.R. & Frenkel, D. (1997). *Science*, **277**, 1975-1978.